Inorganic Chemistry

Article

pubs.acs.org/IC

Concerted Ligand Exchange and the Roles of Counter Anions in the Reversible Structural Switching of Crystalline Peptide Metallo-Macrocycles

Ryosuke Miyake*,[†] and Mitsuhiko Shionoya[‡]

[†]Department of Chemistry and Biochemistry, Graduate School of Humanities and Sciences, Ochanomizu University, 2-1-1 Otsuka, Bunkyo-ku, Tokyo 112-8610, Japan

[‡]Department of Chemistry, Graduate School of Science, The University of Tokyo, 7-3-1 Hongo, Bunkyo-ku, Tokyo 113-0033, Japan

Supporting Information

ABSTRACT: To understand reversible structural switching in crystalline materials, we studied the mechanism of reversible crystal-to-crystal transformation of a tetranuclear Ni^{II} macrocycle consisting of artificial β-dipeptides. On the basis of detailed structural analyses and thermodynamic measurements made in a comparison of pseudo-isostructural crystals (NO_3 and BF_4 salts), we herein discuss how ligand-exchange reactions take place in the crystal due to changes in water content and temperature. Observations of the structural transformation of NO_3 salt indicated that a pseudo crystalline phase transformation takes place through concerted ligand-exchange reactions at the four Ni^{II} centers of the macrocycle with hydrogen bond switching. A mechanism for this ligand exchange was supported by IR spectroscopy. Thermodynamic measurements suggested that the favorable compensation relationship of the enthalpy changes due to water uptake and structural changes are keys to the reversible structural transformation. On the basis of a comparison with the pseudo-isostructural crystals, it is apparent that the crystal packing structure and the types of counter anions are important factors for facilitating reversible ligand exchange with single crystallinity.

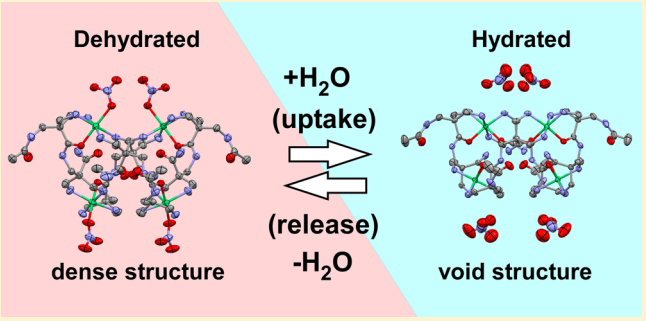

INTRODUCTION

Crystalline materials have great potential for the development of designer functions based on their structural regularity and phase transition characteristics.[1−3] Reversible structural changes of metal-containing crystalline materials caused by external stimuli (light, temperature, molecular adsorption, etc., in particular) are known to enable functional switching with respect to molecular adsorption,[4] spin-state transition,[5] electron conductivity,[6] catalytic reactions,[7] and so on. Metal-centered structural changes in crystal states, such as coordinated geometrical changes[4] and ligand-exchange reactions,[4,8−10] can potentially become keys to such switching behaviors that are observed in metal-containing crystals. However, it is rather difficult to control reversible ligand exchange reactions in a crystal-to-crystal manner under mild conditions.[11] It is, therefore, a challenge to study how to facilitate such structural switching[12] based on proper design.

Recently, we demonstrated that a tetranuclear Ni^{II} macrocycle formed from β-dipeptides (**1**) as NO_3 salt in the crystal state exhibited rapid and reversible crystal-to-crystal transformation by ligand-exchange reactions responsive to non-coordinating guest stimuli (Figure 1).[13] The cooperative structural switching takes place at −40 °C via hydrogen bond switching within the peptide ligands.[14] This transformation accompanies the opening and closing of nano-cavities with rearrangement of the functional groups in the cavity (Figure 1c). Furthermore, the structural changes take place stepwise with changes in water content, as revealed by single-crystal X-ray diffraction and thermodynamic analyses.[13,15]

Herein, we describe a detailed mechanism for this stepwise structural transformation of the crystalline peptide metallo-macrocycle by using X-ray analyses and IR spectroscopy. This study revealed that the structural transformation took place through concerted ligand-exchange reactions within one macrocycle. This transformation was caused by the compensation of enthalpy changes due to structural changes in the macrocycles and by stabilization due to water uptake. The ligand exchange-triggered structural transformation process was well-explained by the effect of crystal packing structure and the different behaviors of counter anions as well as hydrogen bond switching.[13]

RESULTS AND DISCUSSION

Counter Anion Effects on Structural Transformation. To clarify the effects of counter anions on the structural

Received: March 1, 2014
Published: May 14, 2014

   dx.doi.org/10.1021/ic500478p | *Inorg. Chem.* 2014, 53, 5717−5723

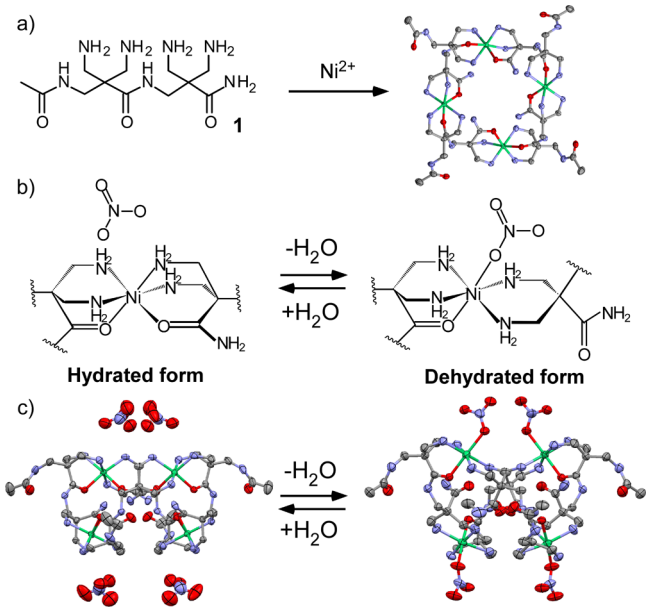

Figure 1. (a) The structure of Ni^{II} macrocycles consisting of artificial β-dipeptide **1**, (b) structural changes at the Ni^{II} center, and (c) the water content-dependent, reversible crystal-to-crystal structural transformation of the macrocycle.[13] Hydrogen atoms are omitted for clarity.

changes, we first examined BF_4^- anions, which have almost the same crystal packing structures as NO_3 salt.[13] As a result, we found that the BF_4 salt of the Ni^{II} macrocycle has almost the same structure as the NO_3 salt. The dipeptide ligand **1** was mixed with an equimolar amount of $Ni(BF_4)_2{\cdot}6H_2O$ in water, and the solution was slowly evaporated at 3 °C[16] to obtain purple prismatic crystals in 50% yield. As shown in Figure 2 and Table 1, the X-ray structural analysis of the resulting single

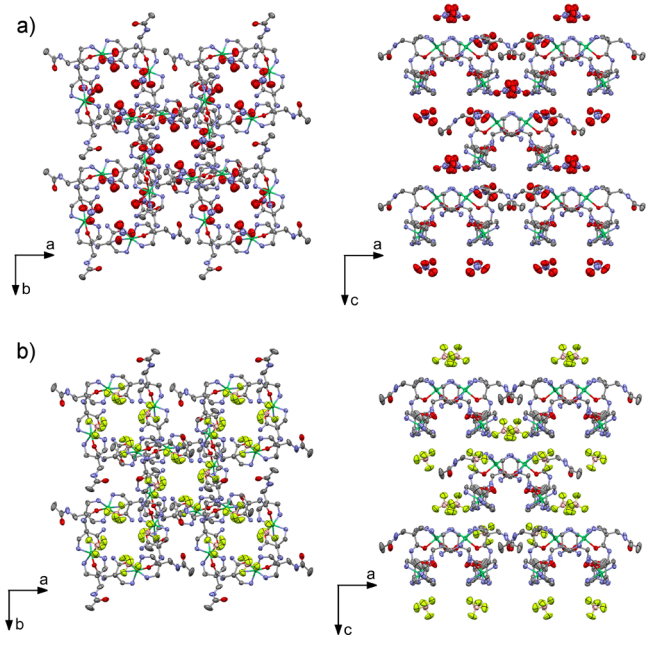

Figure 2. Thermal ellipsoid representation showing the crystal packing structure of $[Ni_4\mathbf{1}_4]^{8+}$ as (a) NO_3 salt[13] and (b) BF_4 salt. Only a few counter anions located near the Ni^{II} centers are shown. The other counter anions, all included water molecules, and hydrogen atoms are omitted for clarity. Thermal ellipsoids are set at 50% probability.

Table 1. Crystal Data for $[Ni_4\mathbf{1}_4]^{8+}$ Obtained at 93 K

	BF_4 salt	NO_3 salt[13]
	$Ni_4\mathbf{1}_4(BF_4)_8{\cdot}12.05H_2O$	$Ni_4\mathbf{1}_4(NO_3)_8{\cdot}11H_2O$
crystal size (mm)	0.29 × 0.20 × 0.15	0.16 × 0.14 × 0.10
formula[a]	$C_{48}H_{131.10}B_8F_{32}N_{28}Ni_4O_{24.05}$	$C_{48}H_{130}N_{36}Ni_4O_{47}$
M[a]	2416.03	2198.72
crystal system	tetragonal	tetragonal
space group	$I\bar{4}$	$I\bar{4}$
a (Å)	15.7021(6)	15.4881(7)
b (Å)	15.7021(6)	15.4881(7)
c (Å)	19.7468(8)	19.3282(9)
α (deg)	90	90
β (deg)	90	90
γ (deg)	90	90
V (Å^3)	4868.7(3)	4636.5(4)
Z	2	2
ρ_{calcd} (g·cm^{-1})	1.648	1.575
$F(000)$	2497	2316
μ (mm^{-1})	0.902	0.912
θ range (deg)	1.66−35.68	2.11−30.03
GOF	1.042	1.060
reflections collected	29091	17487
independent reflections	11191	6693
flack parameter	0.01(2)	0.097(15)
R_{int}	0.0204	0.0189
R_σ	0.0415	0.0363
final $R1$ ($I > 2\sigma(I)$) (all data))	0.0428(0.0511)	0.0507(0.0546)
$wR2$ ($I > 2\sigma(I)$) (all data))	0.1208(0.1276)	0.1476(0.1532)
CCDC No.	973213	856057

[a]For the formula and molecular weight (M), we included hydrogen atoms of water molecules in the crystal, although we did not determine them in the refined structures.

crystal revealed that the BF_4 salt of the Ni^{II} macrocycle had an $I\bar{4}$ crystal system with one-fourth of the molecules being in the asymmetric units. The crystal packing structure of the BF_4 salt was almost the same as that of the NO_3 salt in terms of the positions of the counter anions (Figure 2). The only differences were the disorder pattern of the counter anions and the size of crystal units. Although the positions of the counter anions in the two crystals were almost the same (Supporting Information, Figures S2 and S3), BF_4^- ions were disordered more significantly than NO_3^- ions, suggesting that the NO_3^- ions interacted closely with the framework of the peptide metallomacrocycle through hydrogen bonding. In addition, the BF_4 salt was a little larger in the c-axis direction compared with the NO_3 salt.

First, we compared the structural changes in these pseudo-isostructural crystals by removing the included water molecules. As shown in Figure 3, the water-release processes revealed by X-ray single-crystal analysis were similar to each other and included water molecules in contact with both counter anions and the dipeptide ligand (Supporting Information, Table S1). During the heating process to 40 °C, both the NO_3 and BF_4 salts exhibited almost the same structural changes, with similar water-release processes involving the migration of neighboring macrocycles. In contrast, the crystal structural changes from 40 to 60 °C were completely different from each other. In the BF_4

dx.doi.org/10.1021/ic500478p | Inorg. Chem. 2014, 53, 5717−5723

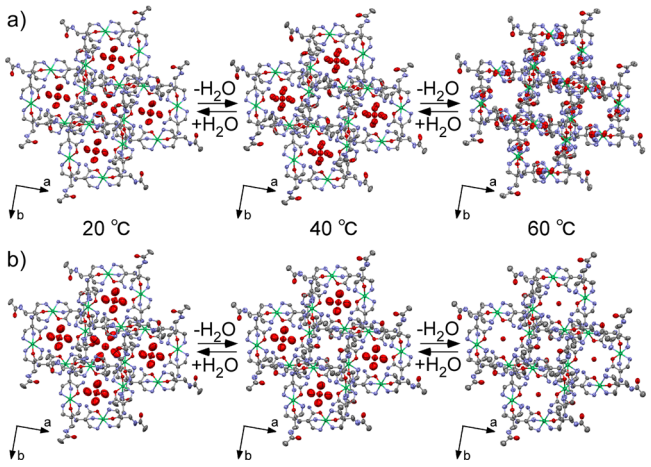

Figure 3. Comparison of temperature-dependent changes in the single crystal structures between (a) NO_3 salt[13] and (b) BF_4 salt at 20, 40, and 60 °C. Counter anions and hydrogen atoms are omitted for clarity.

salt crystal, one water molecule per macrocycle still remained after heating to 60 °C. In contrast, all of the water molecules were removed in the case of the NO_3 salt, and the crystal-to-crystal structural transformation was accompanied by ligand-exchange motions between a terminal amide oxygen of **1** and an oxygen atom of an NO_3^- anion. As a result of the structural changes, the nanochannel structure in the hydrated form was converted to a dense structure in the dehydrated form. Because of a decrease in the single crystallinity above 100 °C, the BF_4 salt was analyzed by X-ray powder diffraction to determine the crystal structure after removing all of the included water molecules. The analysis was performed at room temperature under dry conditions after the sample was dried at 200 °C in vacuo for 1 h.[17] As shown in Figure 4, no peak shifts, although

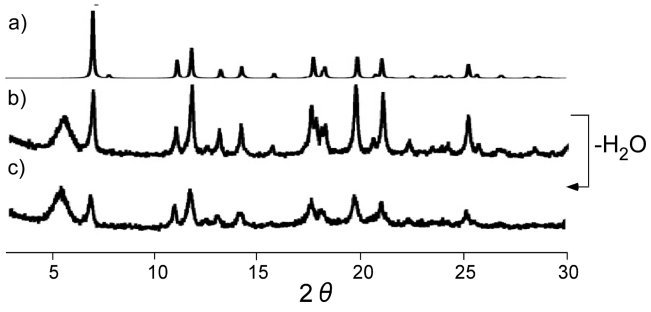

Figure 4. Powder diffraction patterns of the BF_4 salt. (a) A simulated pattern of the hydrated form. (b) A pattern of the as-synthesized sample. (c) A pattern of the sample dried at 200 °C in vacuo. All diffraction patterns were measured under an Ar atmosphere at 20 °C using a sealed cell. The broad peaks observed at around 5° represent the scattering of the kapton film of the cell.

they were slightly broadened, were observed for the dried BF_4 salt, while the dried NO_3 salt showed significant peak shifts as shown in Figure 5. Thus, only a slight difference between the BF_4^- and NO_3^- ions caused the different structural transformation behaviors.

We then compared the dehydration (water release) processes by thermogravimetric analysis (Supporting Information, Figure S4). The BF_4 salt showed a stepwise weight loss with the rising temperature, as was also observed for the NO_3 salt. It is noteworthy that their water-release processes were almost

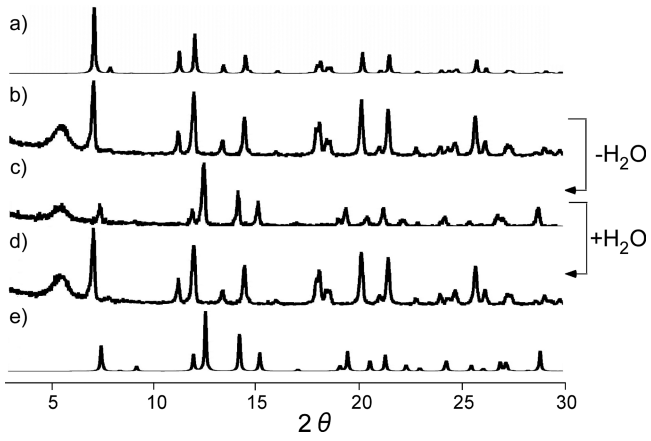

Figure 5. Powder diffraction patterns of the NO_3 salt: (a) a simulated pattern of the hydrated form, (b) the as-synthesized sample, (c) after being dried at 60 °C in vacuo, (d) after water uptake, and (e) a simulated pattern of the dehydrated form. All diffraction patterns were measured under dry Ar gas at 20 °C using a sealed cell. The broad peaks observed at around 5° represent the scattering of the kapton film of the cell.

identical up to ca. 60 °C, suggesting that the counter anions slightly affected the water-release processes. As was also suggested by the X-ray structural analysis, more than one water molecule per one macrocycle of the BF_4 salt still remained at around 60 °C, but the dehydration was completed at around 200 °C. However, a differential scanning calorimetry (DSC) analysis showed that the BF_4 salt exhibited only one broad and small endothermic peak (Supporting Information, Figures S5 and S6), whereas the NO_3 salt showed one relatively broad peak for the first step water weight loss and a sharp endothermic peak (Figure 6).[13] This result also suggests that there were no significant structural changes in the BF_4 salt.

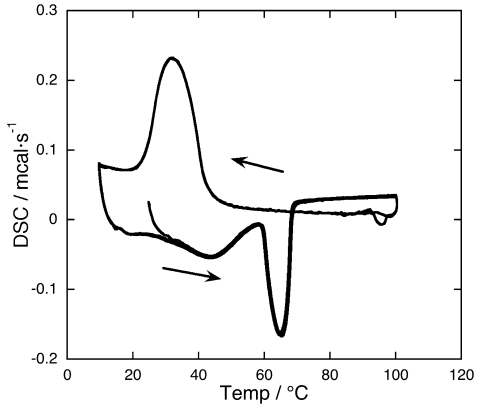

Figure 6. DSC curves for $Ni_4\mathbf{1}_4(NO_3)_8$ measured under N_2 gas containing water vapor at a pressure of 8.8 hPa with a repetitive process of heating and cooling.

Structural Transformation by Thermodynamic Study. Although coordination of BF_4^- ions to Ni^{II} ions is well-known,[18] no ligand-exchange reactions took place in the BF_4 salt crystal as described above. To clarify the reasons for the smooth and reversible ligand exchanges in the NO_3 salt, we studied the origin of the reversible structural transformation by using thermodynamic parameters. Since the DSC peaks of the BF_4 salt were too broad to estimate the parameters, we then tried to investigate the ligand-exchange reactions by further

dx.doi.org/10.1021/ic500478p | Inorg. Chem. 2014, 53, 5717−5723

thermodynamic study of NO_3 salt. We first examined the reversibility of the NO_3 salt by a repetitive process of heating and cooling under N_2 gas mixed with 8.8 hPa water vapor. As shown in Figure 6, the repeated DSC curves are highly overlapped with each other. The sharp peaks, which are assignable to the peaks for the transformation between the hydrated form and the dehydrated form, exhibited hysteresis. This agreed well with previously reported results:[13] the peaks showed high dependency on water vapor pressure, which can be explained by the Clausius−Clapeyron equation, and strongly suggested that, from the viewpoint of the states of the water molecules, this phenomenon can be regarded as a pseudo phase transition between the inclusion phase and the gas phase of the water molecules.[19] The vaporization enthalpy of water (ΔH_{vap}) was estimated to be 57 kJ mol^{-1} per one water molecule by this equation.[13] On the other hand, the total peak area for the heating process was equal to that of the cooling process. These peak areas indicated the total enthalpy changes of the structural transformation, including enthalpy changes due to the structural changes (ΔH_{str}) and water release (uptake) which was already estimated as a value per one water molecule. Since the same number of water molecules (i.e., four molecules per one macrocycle[13]) induced the structural transformation, we can estimate ΔH_{str} approximately by comparing the two thermodynamic parameters (DSC peak area and vaporization enthalpy). The enthalpy changes during vaporization of water molecules should be 2.3×10^2 kJ mol^{-1} (i.e., 4×57 kJ mol^{-1}) per one macrocycle.[13] In contrast, the total enthalpy determined by the DSC analysis (1.5×10^2 kJ mol^{-1}) was smaller than that.[20] This strongly suggests that the change in structural enthalpy (ΔH_{str}) for the structural transformation accompanied by the water release is negative (ca. -8×10 kJ mol^{-1}); that is, the crystal lattice of the dehydrated form is much more stable than that of the hydrated form. This result also agrees well with the fact that the NO_3 salt easily released all included water molecules at a relatively low temperature (above −40 °C[13]), although the large ΔH_{vap} value suggested high stabilization of the included water molecules. In contrast, the transformation in the opposite direction, that is, transformation from the dehydrated to the hydrated form, also readily occurred on exposure to an ambient atmosphere that included a small amount of water vapor. Since the enthalpy change during the vaporization of one water molecule was large in this system, the uptake of one or two water molecules per macrocycle was needed to overcome the disadvantage of structural enthalpy for the ligand exchange from the hydrated to the dehydrated form. Thus, the favorable balance between the changes in structural enthalpy (ΔH_{str}) and vaporization (adsorption) enthalpy of water (ΔH_{vap}) was important in facilitating the reversible structural changes.

The thermodynamic parameters also support the reason for the difference in the structural changes between the NO_3 and BF_4 salts described above. Since they exhibited similar water-release processes, the difference should be responsible for the enthalpy changes in the structural changes (i.e., ΔH_{str}). The most likely possible differences affecting structural enthalpy are the coordination abilities of the counter anions and the crystal-packing structures. Therefore, the negligibly small structural change in the BF_4 salt, even after removing all of the included water molecules, was probably due to the weaker coordination ability of the BF_4^- ions compared with the NO_3^- ions and to the slightly larger size of the BF_4^- ions than the NO_3^- ions for dense packing structures.

Observation of the Structural Transformation Processes in the NO_3 Salt. Then, we further analyzed the structural transformation processes of the NO_3 salt by time-course powder X-ray diffraction (PXRD) and IR spectroscopy. The powder patterns of the NO_3 salt varied with humidity (Figure 5). Diffraction patterns of as-synthesized NO_3 salt (hydrated form) and dried NO_3 salt (dehydrated form) agreed well with those calculated from their single-crystal structures. The structural transformation process was successfully observed as changes in the diffraction patterns with the slow increase in humidity due to the air leak from a sealed cell (Figure 7 and Supporting Information, Figure S8). With an increase in humidity in the cell, the peak intensity of the dehydrated form gradually decreased, and new peaks appeared in 1 h. Then, the diffraction peaks of the dehydrated form eventually disappeared within 1.5 h. After 3 d, a further peak shift was observed. The final powder pattern was consistent with that of the as-synthesized NO_3 salt. Considering that the simulated powder patterns of the NO_3 salt at 20 and 40 °C were similar to each other, the latter peak shift can be assigned to the first structural change in Figure 3a (migration of neighboring macrocycles). The changes in the two diffraction peaks during the transformation with the ligand-exchange reactions were observed without any apparent decrease in intensity. Thus, this result strongly suggests that the transformation takes place with cooperative ligand-exchange reactions between the two states, the dehydrated form and the hydrated form, within the macrocycle without forming any detectable intermediates (Figure 8).

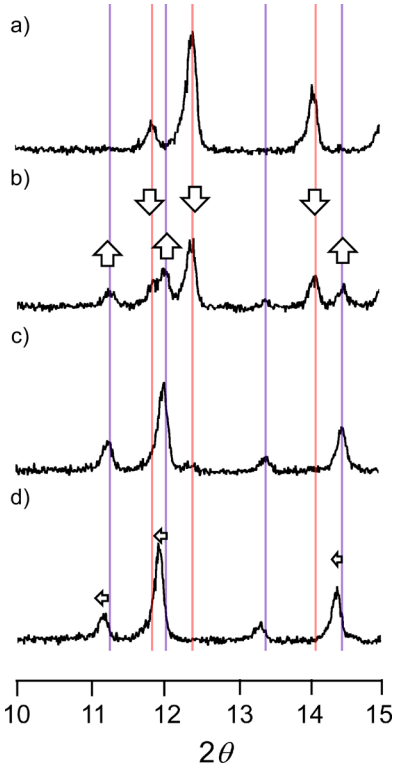

Figure 7. (a) Powder diffraction patterns of the NO_3 salt ($I\bar{4}$) showing a two-stage structural change in the water uptake process: (a) dried sample measured under dry Ar gas, and time-course analyses of the structural changes following a slow increase in humidity in the cell after (b) 1 h, (c) 1.5 h, and (d) 3 d.

dx.doi.org/10.1021/ic500478p | Inorg. Chem. 2014, 53, 5717−5723

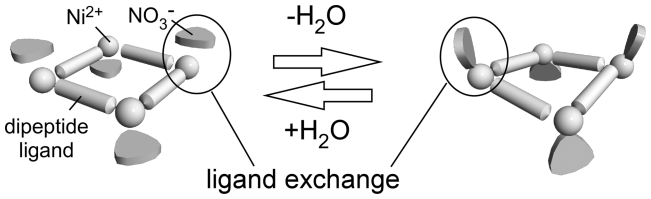

Figure 8. Schematic representation of the structural transformation process with ligand-exchange reactions.

The structural changes were further studied by IR spectroscopy to verify the changes in the chemical environment of the individual functional groups during the slow water-uptake process as analyzed by the PXRD measurements.[21] As shown in Figure 9 and Supporting Information, Figure S9, apparent peak

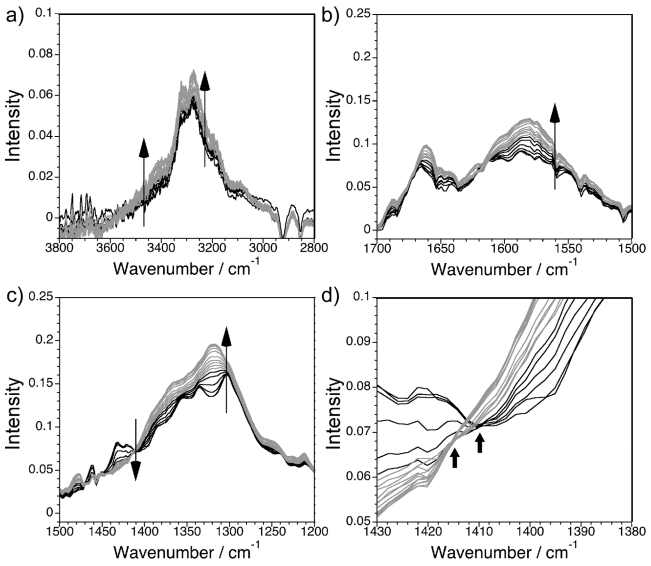

Figure 9. IR spectral changes of dried NO_3 salt undergoing a slow water-uptake process. (a) OH vibration region (3800−2800 cm^{-1}). (b) CO vibration region (1700−1500 cm^{-1}). (c) NO vibration region (1500−1300 cm^{-1}). (d) Extended figure around the isosbestic points. IR spectra are shown with black lines (the first half part) and gray lines (the latter half part).

changes were observed in the peak area ascribable to ligand-exchange reactions: the hydroxyl group of water molecules (3600−3300 cm^{-1}), the amide carbonyl groups of the ligands (1650−1550 cm^{-1}), and the nitrate groups (1400−1300 cm^{-1}). The sharp peak at 1428 cm^{-1} was observed only for the dehydrated form. This peak is attributable to the NO_3^- anion bound to the Ni^{II} center.[22] In the time-course measurement, the stepwise structural transformation was also observed in the IR spectra both in the water-uptake (Figure 9) and water-release processes (Supporting Information, Figure S9). In the region of the stretching vibrations of the hydroxyl groups (3600−3300 cm^{-1}), a broadened peak emerged at around 3400 cm^{-1} with water uptake. In contrast, for the peaks in the amide and nitrate regions at around 1580 and 1300 cm^{-1}, respectively, several split peaks changed to one broadened peak (Figure 9 and Supporting Information, Figure S9). Interestingly, the spectrum in the nitrate region (1400−1300 cm^{-1}) changed, with isosbestic points indicating a two-stage process for ligand exchange and migration (black and gray lines were used for each stage in Figure 9d). This result is consistent with the two-stage structural change suggested by the single-crystal and powder X-ray analyses.

To gain a better understanding of the details of the transformation process, the changes in the absorbances at 3413 cm^{-1} (included water molecules), 1582 cm^{-1} (amide carbonyl), 1428 cm^{-1} (coordinated NO_3^-), and 1320 cm^{-1} (NO_3^-) were plotted against time, as shown in Figure 10. For

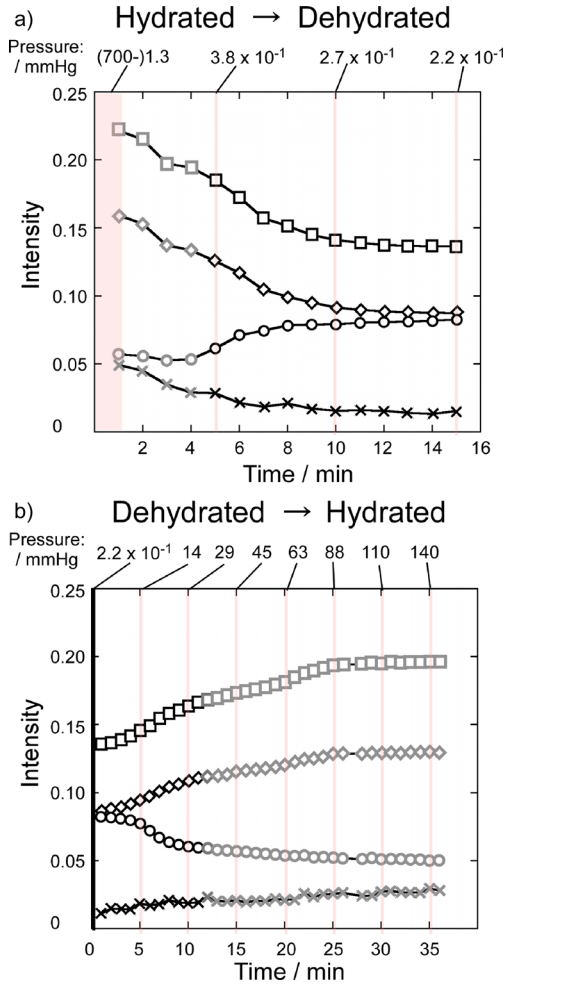

Figure 10. Changes over time in IR absorbance for each peak in (a) the water-release process (Supporting Information, Figure S9) and (b) the water-uptake process (Figure 9). 3413 cm^{-1}: ×, 1580 cm^{-1}: ◇, 1431 cm^{-1}: ○, 1318 cm^{-1}: □. The observed pressure of the measured cell is shown above for selected data.

comparison with Figure 9, the data are colored differently to distinguish the two-stage process for ligand exchange and migration. Since the structural changes were triggered by water uptake/release, other vibration regions in the IR spectra also follow the changes in the water (O−H) vibration region. However, the peak changes at 1428 cm^{-1} for coordinated NO_3^- ions were seen only at the beginning of the structural transformation with ligand exchange. This implies that concerted ligand exchange was involved at the Ni^{II} centers, leading to the structural transformation.

■ CONCLUSION

In summary, we revealed the detailed crystal-to-crystal structural changes that occur in crystalline Ni^{II} macrocycles with β-dipeptide and the effects of counter anions on the

dx.doi.org/10.1021/ic500478p | Inorg. Chem. 2014, 53, 5717−5723

process. The distinct reversible transformation was caused by compensation for the large degree of stabilization due to water uptake and changes in structural stability in the transformation. The structural transformation process involved concerted ligand-exchange reactions in the macrocyclic structure, which led to a two-state transformation. The ligand-exchange behaviors were strongly affected by the types of counter anions, even in the same crystal-packing structures (NO_3 vs BF_4 salts). Both PXRD and IR analyses confirmed the two-stage process, migration of neighboring macrocycles and ligand exchange, between the hydrated form and the dehydrated form. This dynamic structural transformation caused by the water content in the crystal state was most likely realized by the structurally flexible peptide and its ability to form a hydrogen bonding network. Such indirect control of ligand-exchange reactions in the crystal state by external stimuli provides a clue to developing a new type of functional materials.[23]

EXPERIMENTAL SECTION

Dipeptide ligand **1**·(CF_3CO_2H) was synthesized according to a previously reported method.[15] All reagents and solvents were used without further purification. Differential scanning calorimetry (DSC) measurements were conducted using a Bruker DSC 3100SA under ambient pressure of N_2 gas at a scanning rate of 1 °C min^{-1}. Thermogravimetric (TG) analysis was performed using a Bruker TG-DTA 2000SA under ambient pressure of N_2 gas at a scanning rate of 1 °C min^{-1}. Crystallographic data were collected using a Bruker APEXII CCD detector with Mo Kα radiation (λ = 0.710 75 Å). The structures were solved by direct methods using the program SHELXS. The refinement (on F^2) and graphical calculations were performed using the SHELIXL program suite.[24,25] For the measurements at normal humidity, samples were set up in glass capillaries. BF_4^- anions were refined by using SADI (between B and F), SIMU, and ISOR restraints, and water molecules were refined by using SIMU and ISOR restraints. In addition, SUMP restraints were used for hardly disordered BF_4^- anions to fix the sum of their occupancy. For the details, see the Supporting Information.

IR spectroscopic measurements were carried out using a Mettler Toledo reactIR 4000. Samples were set on a measurement window and closely sealed using a three-neck flask at room temperature. The measurements were performed in vacuo while monitoring the inner pressure. The PXRD patterns were measured using a Rigaku Ultima IV. For the observations of the structural transformations controlled by the water content, dried samples were used in a sealed cell (Quick air tight sample attachment (Rigaku Co. Ltd.)) under an Ar atmosphere. Elemental analysis was carried out using a Yanaco CHN corder MT-6.

SYNTHESIS OF $Ni_4\mathbf{1}_4(BF_4)_8·12H_2O$

1·(CF_3CO_2H)$_4$ (309 mg, 400 μmol) was neutralized by anion exchange column chromatography (IRA-400) to produce acid-free β-dipeptide **1** as a colorless syrup. $Ni(BF_4)_2·6H_2O$ (136 mg, 400 μmol) in H_2O (1 mL) was added to a solution of the acid-free **1** in H_2O (2 mL). After slow evaporation of water at 3 °C to prevent hydrolysis of BF_4^- ions, the resulting purple prismatic crystals were collected by filtration and dried in air to afford Ni^{II} complex (120 mg, 50%); melting point = 296.5−297.1 °C (dec). IR 3356, 1660, 1588, 1019 cm^{-1}. Anal. Calc for $C_{48}H_{132}B_8F_{32}N_{28}Ni_4O_{24}$ ($Ni_4\mathbf{1}_4(BF_4)_8(H_2O)_{12}$): C, 23.87; H, 5.51; N, 16.24. Found: C, 24.25; H, 5.65; N, 16.61%.

ASSOCIATED CONTENT

Supporting Information

Additional structural data, and spectral data for the peptide macrocycles with additional discussion about the structural transformation. This material is available free of charge via the Internet at http://pubs.acs.org. Crystallographic data can be obtained free of charge from the Cambridge Crystallographic Data Centre via www.ccdc.cam.ac.uk/data_request/cif (CCDC 973213−973219).

AUTHOR INFORMATION

Corresponding Author

*E-mail: miyake.ryosuke@ocha.ac.jp.

Notes

The authors declare no competing financial interest.

ACKNOWLEDGMENTS

This study was partly supported by a Grant-in-Aid for Scientific Research (S) to M.S. (Grant No. 21225003) and a Grant-in-Aid for Young Scientists (B) to R.M. (Grant No. 25810037) from the Ministry of Education, Culture, Sports, Science, and Technology of Japan. We thank Prof. Masanobu Uchiyama and Mr. Kengo Yoshida (The Univ. of Tokyo) for IR measurements, Ms. Chika Kuwata (Ochanomizu Univ.) for assistance with complex preparation, and Prof. Yuichi Masuda and Dr. Yukie Mori (Ochanomizu Univ.) for helpful discussions.

REFERENCES

(1) Schmidt, G. M. J. *Pure Appl. Chem.* **1971**, *27*, 647 and references therein.

(2) Ohashi, Y. *Acta Crystallogr. A* **1998**, *54*, 842−849 and references therein.

(3) (a) Vittal, J. J. *Coord. Chem. Rev.* **2007**, *251*, 1781−1795. (b) Kole, G. K.; Vittal, J. J. *Chem. Soc. Rev.* **2013**, *42*, 1755−1775. (c) Dalgarno, S. J.; Thallapally, P. K.; Barbour, L. J.; Atwood, J. L. *Chem. Soc. Rev.* **2007**, *36*, 236−245. (d) Braga, D.; D'Agostino, S.; Grepioni, F.; Gandolfi, M.; Rubini, K. *Dalton Trans.* **2011**, *40*, 4765−4777.

(4) (a) Barbour, L. J. *Aust. J. Chem.* **2006**, *59*, 595−596. (b) Halder, G. J.; Kepeert, C. J. *Aust. J. Chem.* **2006**, *59*, 597−604. (c) Ferey, G. *Chem. Soc. Rev.* **2008**, *37*, 191−214. (d) Kitagawa, S.; Uemura, K. *Chem. Soc. Rev.* **2005**, *34*, 109−119. (e) Furukawa, S.; Sakata, Y.; Kitagawa, S. *Chem. Lett.* **2013**, *42*, 570−576.

(5) For recent reviews, see: (a) Sato, O. *Acc. Chem. Res.* **2003**, *36*, 692−700. (b) Hakrow, M. A. *Chem. Soc. Rev.* **2008**, *37*, 278−289. (c) Hayashi, S.; Komatsu, Y.; Shimizu, T.; Kamihara, H.; Lee, H. Y. *Coord. Chem. Rev.* **2011**, *255*, 1981−1990. (d) Ohkoshi, S.; Tokoro, H. *Acc. Chem. Res.* **2012**, *45*, 1749−1758.

(6) (a) Fume, Y.; Ebihara, M.; Kutsumizu, S.; Kawamura, T. *J. Am. Chem. Soc.* **2004**, *126*, 12238−12239. (b) Iguchi, H.; Takaishi, S.; Miyasaka, H.; Yamashita, M.; Matsuzaki, H.; Okamoto, H.; Tanaka, H.; Kuroda, S. *Angew. Chem., Int. Ed.* **2010**, *49*, 552−555.

(7) Ma, L.; Lin, W. *Top. Curr. Chem.* **2010**, *293*, 175−205.

(8) For examples of reversible single-crystal to single-crystal transformation induced by coordination of guest stimuli: (a) Takaoka, K.; Kawano, M.; Tominaga, M.; Fujita, M. *Angew. Chem., Int. Ed.* **2005**, *44*, 2151−2154. (b) Chen, C.-L.; Goforth, A. M.; Smith, M. D.; Su, C.-Y.; zur Loye, H.-C. *Angew. Chem., Int. Ed.* **2005**, *44*, 6673−6677. (c) Zhang, Y.-J.; Liu, T.; Kanegawa, S.; Sato, O. *J. Am. Chem. Soc.* **2010**, *132*, 912−913. (d) Du, M.; Li, C.-P.; Wu, J.-M.; Guo, J.-H.; Wang, G.-C. *Chem. Commun.* **2011**, *47*, 8088−8090. (e) Lin, H.; Maggard, P. A. *Inorg. Chem.* **2009**, *48*, 8940−8946. (f) Ohkoshi, S.; Arai, K.; Sato, K.; Hashimoto, K. *Nat. Mater.* **2004**, *3*, 857−861.

(9) For examples of reversible singe-crystal to single-crystal structural transformation induced by ligand exchange reactions with coordinating small guest stimuli: (a) Huang, Z.; White, P. S.; Brookhart, M. *Nature* **2010**, *465*, 598−601. (b) Lturrospe, A.; Artetxe, B.; Reinoso, S.; San Felices, F. L.; Vitoria, P.; Lezama, L.; Gutierrez-Zorrilla, J. M. *Inorg. Chem.* **2013**, *52*, 3084−3093. (c) Sharma, M. K.; Bharadwaj, P. K.

Inorg. Chem. **2011**, *50*, 1889−1897. (d) Das, M. C.; Bharadwaj, P. K. *Chem.—Eur. J.* **2010**, *16*, 5070−5077.
(10) For recent examples with PXRD: (a) Sun, J.; Dai, F.-N.; Yuan, W.-B.; Bi, W.-H.; Zhao, X.-L.; Sun, W.-M.; Wang, G.-C. *Angew. Chem., Int. Ed.* **2011**, *50*, 7061−7064. (b) Pinkowicz, D.; Podgajny, R.; Gawet, B.; Lacocha, W.; Oszajica, M.; Czapla, M.; Makararewicz, M.; Balanda, M.; Sieklucka, B. *Angew. Chem., Int. Ed.* **2011**, *50*, 3973−3977. (c) Strasser, C. E.; Catalano, V. J. *J. Am. Chem. Soc.* **2010**, *132*, 10009−10011.
(11) (a) Bradshaw, D.; Warren, J. E.; Rosseinsky, M. J. *Science* **2007**, *315*, 977−980. (b) Hu, C.; Englert, U. *Angew. Chem., Int. Ed.* **2005**, *44*, 2281−2283. (c) Seo, J.; Bonneau, C.; Matsuda, R.; Tanaka, M.; Kitagawa, S. *J. Am. Chem. Soc.* **2011**, *133*, 9005−9013.
(12) Recent examples of detailed observation and discussion of simple structural transformation in crystal: (a) Warren, M. R.; Brayshaw, S. K.; Johnson, A. L.; Schiffers, S.; Raitnby, P. R.; Easun, T. L.; George, M. W.; Warren, J. L.; Teat, S. J. *Angew. Chem., Int. Ed.* **2009**, *48*, 5711−5714. (b) Kondo, A.; Nakagawa, T.; Kajiro, H.; Chinen, A.; Hattori, Y.; Okino, F.; Ohba, T.; Kaneko, K.; Kanoh, H. *Inorg. Chem.* **2010**, *49*, 9247−9252. (c) Mahata, P.; Ramya, K. V.; Natarajan, S. *Inorg. Chem.* **2009**, *48*, 4942−4951. (d) Takamizawa, S.; Nakata, E.; Akatsuka, T.; Miyake, R.; Kakizaki, Y.; Takeuchi, H.; Maruta, G.; Takeda, S. *J. Am. Chem. Soc.* **2010**, *132*, 3783−3792. (e) Sarma, D.; Natarajam, S. *Cryst. Growth Des.* **2011**, *11*, 5415−5423. (f) Marti-Rujas, J.; Kawano, M. *Acc. Chem. Res.* **2013**, *46*, 493−505.
(13) Miyake, R.; Shionoya, M. *Chem. Commun.* **2012**, *48*, 7553−7555.
(14) There are some examples of peptide-based structural switching in solution. For example, see: Tashiro, S.; Shionoya, M. *Chem. Lett.* **2013**, *42*, 456−462.
(15) Miyake, R.; Tashiro, S.; Shiro, M.; Tanaka, K.; Shionoya, M. *J. Am. Chem. Soc.* **2008**, *130*, 5646−5647.
(16) The solution should be kept at 3 °C to avoid hydrolysis of BF_4^- ions and generation of F^- ions. In the presence of F^- ions, the resulting crystals of Ni(II) macrocycles include a F^- ion in each hole.
(17) TG measurements of the BF_4 salt suggest that the included water molecules can be removed at 200 °C. For the details, see Supporting Information (Figure S4).
(18) For examples: (a) Yeh, C.-Y.; Chiang, Y.-L.; Lee, G.-H.; Peng, S.-M. *Inorg. Chem.* **2002**, *41*, 4096−4098. (b) Arakawa, M.; Suzuki, N.; Kishi, S.; Hasegawa, M.; Satoh, K.; Horn, E.; Fukuda, Y. *Bull. Chem. Soc. Jpn.* **2008**, *81*, 127−135.
(19) A similar discussion was described in ref 12d.
(20) Since the sample weight changed slightly (∼5%) due to the release/uptake of water molecules, the estimated enthalpy from the DSC peak area included up to ca. 10% error. The reference values are shown in the manuscript to help understand this.
(21) Different cells were used for PXRD and IR measurements. Therefore, the rates of increasing humidity inside the cells were completely different in both experiments.
(22) Davis, A. R.; Irish, D. E. *Inorg. Chem.* **1968**, *7*, 1699−1704.
(23) For examples of studies on conformational dynamics using crystals of simple peptides: (a) Anedda, R.; Soldatov, D. V.; Moudrakovski, I. L.; Casu, M.; Ripmeester, J. A. *Chem. Mater.* **2008**, *20*, 2908−2920. (b) Rabone, J.; Yue, Y.-F.; Chong, S. Y.; Stylianou, K. C.; Bacsa, J.; Bradshaw, D.; Darling, G. R.; Berry, N. G.; Khimyak, Y. Z.; Gnin, A. Y.; Wiper, P.; Claridge, J. B.; Rosseinsky, M. J. *Science* **2010**, *329*, 1053−1057. (c) Martí-Gastaldo, C.; Warren, J. E.; Stylianou, K. C.; Flack, N. L. O.; Rosseinsky, M. J. *Angew. Chem., Int. Ed.* **2012**, *51*, 11044−11048.
(24) Sheldrick, G. M. *SHELXL-97*, Program for refinement of crystal structures; University of Göttingen: Gottingen, Germany, 1997.
(25) Sheldrick, G. M. *SADABS*, Program for scaling and correction of area detector data; University of Göttingen: Gottingen, Germany, 1996.

dx.doi.org/10.1021/ic500478p | *Inorg. Chem.* 2014, 53, 5717−5723